Major stable surface of silicon: Si(20 4 23)

Zheng Gai,[1,2] R. G. Zhao,[1] Wenjie Li,[1] Y. Fujikawa,[2] T. Sakurai,[2] and W. S. Yang[1,*]
[1]*Mesoscopic Physics Laboratory and Department of Physics, Peking University, Beijing 100871, China*
[2]*The Institute for Materials Research (IMR), Tohoku University, Sendai 980-8577, Japan*
(Received 11 July 2000; revised manuscript received 12 April 2001; published 4 September 2001)

Clean and well-annealed Si(515), (516), and (405) surfaces have been investigated by means of scanning tunnel microscope (STM) and low-energy electron diffraction and it turns out that these surfaces are unstable while Si(20 4 23) is stable, because the former three all consist of {20 4 23} facets. On the basis of the high-resolution dual-bias STM images of the Si(20 4 23)1×1 surface, a detailed structural model of the surface has been proposed for further investigation. As the unit cell of the Si(20 4 23) surface has its own structure rather than consisting of nanofacets of other stable surface(s) the surface is identified, by definition, as a major stable surface (or MAJOR). Interestingly, among all MAJOR's of silicon that have been found so far (20 4 23) is the only one that silicon does not share with germanium.

DOI: 10.1103/PhysRevB.64.125201 PACS number(s): 68.35.Bs, 68.37.Ef, 61.14.Hg

I. INTRODUCTION

The rapid development of nanotechnology has made high-index surfaces of elemental semiconductors increasingly important, because heterogeneous nanostructures such as quantum dots and wires grown on Si(001) substrates are often made up of stable high-index facets[1] and they can grow as well on some stable high-index substrates like Si(313).[2] Moreover, faceting of unstable high-index surfaces may result in quite regular mesoscopic or nanoscale surface patterns[3,4] and thus may provide natural templates for growth of nanostructures.[5–7] For germanium, through a series of recent investigations, it has been known that there is a total of 14 stable surfaces and that seven among them are major stable surfaces (MAJOR) while the rest are minor stable surfaces [MINOR, see Fig. 1(a)].[4] The difference between MAJOR's and MINOR's is that the unit cell of any MINOR is faceted to nanofacets of one or more MAJOR's.[8] All other germanium surfaces are unstable and after being well annealed are faceted to facets of one or more stable surfaces, either MAJOR's or MINOR's. For silicon surfaces, extensive investigation has been carried out for several decades and, as a result, understanding of the structure of the most-important low-index Si surfaces, (001) and (111), as well as their vicinal surfaces has become quite comprehensive.[9] However, only very recently the structure of the most-stable high-index surface Si(113) has been disclosed,[10] and models have been proposed for the Si(5 5 12),[11] (112),[12] and (114)[13] surface. Apart from these, till not long ago it was only known that Si(313) (Ref. 14) and (101) (Ref. 15) are also stable, but no detailed structural models had been proposed for them. As for surfaces inside the unit stereographic triangle only little has been known, except that Si(15 3 23) likely is a stable surface.[16] Only very recently, it has been known that Si(103) and (105) are both MINOR's but have unique morphologies,[17,18] that Si(313) is a MAJOR and its well-annealed surface is (12×1) reconstructed and metallic,[19] and that Si(15 3 23) is not only stable but also a MAJOR.[20] In the present paper, we study silicon surfaces surrounded by (101), (313), and (15 3 23) in the stereographic triangle [see Fig. 1(b)] and have found that Si(20 4 23), which had never been reported before, is a MAJOR. Interestingly, for germanium (20 4 23) is not a MAJOR although silicon and germanium share, at least, six MAJOR's (see Fig. 1).

II. EXPERIMENT

The scanning tunnel microscope (STM) part of the experiment was carried out in the UHV system that is equipped with STM, low-energy electron diffraction (LEED), and AES (Auger electron spectroscopy), as well as ion bombardment and annealing facilities.[21] The LEED part was performed in the UHV system that is equipped with LEED, AES, and electron energy loss spectroscopy, as well as ion bombardment and annealing facilities.[22] Both systems were used recently.[4] In the STM experiment the bias voltage is applied to the sample and the tip is grounded. Throughout the experiment the constant-current mode was used. The images shown here were acquired with either the ac mode or the dc mode, which are the same as the ac and dc input mode of oscilloscopes, respectively. The ac mode in STM experiment is also called local-contrast enhanced mode. The tip was made out of a thin [111]-W single crystal with electrochemical etching. The Si(515), (516), and (405) samples were cut with a precision of $\pm1°$ from a silicon single-crystal rod (p doped, 6–8 Ωcm) and were subjected to several cycles of "argon-ion bombardment plus subsequent annealing at 1000 °C" followed by slow cooling (2 °C/sec) to room temperature so that a clean and well-annealed surface was obtained prior to LEED and STM observations.

III. OBSERVATION

The well-annealed Si(515) surface is completely faceted as shown by our LEED and STM data, and thus is an unstable surface. A typical LEED pattern is given in Fig. 2(a). The pattern has a mirror plane at $(1\ 0\ -1)$ and two (0 0) diffraction spots, which can be identified by varying the energy of the incidence electron beam. This fact indicates not only that the surface consists of two sets of facets but also that $(1\ 0\ -1)$ is the mirror plane of the two. This in turn makes us able to find out which spots belong to which set of

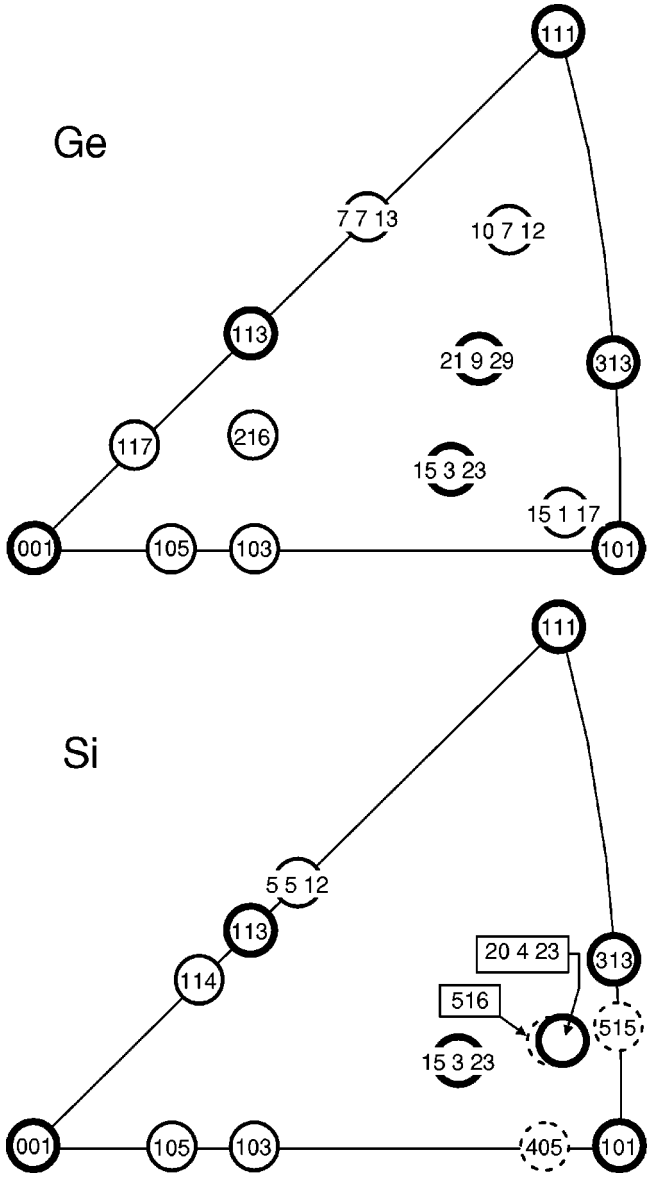

FIG. 1. (a) Unit stereographic triangle of germanium, showing all-seven major stable surfaces (MAJOR, thick circles) and all-seven minor stable surfaces (MINOR, thin circles) (b) Same as (a) but for silicon, showing the MAJORs and MINORs found so far, as well as the three unstable surfaces (dotted circles) studied in the present paper: (515), (516), and (405). The assignment of Si(114) to MAJOR is based on Ref. 13 while that of (5 5 12) to MINOR is based on Ref. 11, and thus both are temporal.

facets, as well as the reciprocal space-unit vectors. According to the lengths of the vectors and the angles the vectors form, the facets have been identified as (20 4 23) and (23 4 20). The simulated LEED pattern based on this assignment is given in Fig. 2(b) and it is indeed in good agreement with the real pattern. To show that this assignment is also supported by our STM observation, a typical low- and medium-magnification STM image of the surface is given in Figs. 3(a) and 3(b), respectively. The lengths and relative orientations of the real space-unit vectors are, as one can see, indeed in excellent agreement with their counterpart calculated from the reciprocal space-unit vectors determined with LEED. We note that Si(35 7 47), which is 4.4° away from (20 4 23), was reported by Olshanetsky and Shklyaev as a stable surface.[23] We believe, however, what they found was actually Si(20 4 23) rather than (35 7 47), because they used only LEED and the [(35 7 47) + (47 7 35)] LEED pattern can really be of quite confusion with the [(20 4 23) + (23 4 20)] pattern, if not looked at it very carefully. Thus we conclude that a well-annealed Si(515) surface facets to (20 4 23) facets, although the angle between the two planes is 4.0°.

To make sure that Si(20 4 23) is indeed a stable surface, by means of LEED, we have also studied Si(516) and (405), which are 1.2° and 7.8° away from (20 4 23), respectively [see Fig. 1(b)]. It turned out that, after being well annealed, the former faceted only to (20 4 23) facets [see Fig. 2(c)] whereas the latter to (20 4 23) and (20 −4 23) facets [see Fig. 2(d)]. These results show that Si(20 4 23) not only is indeed stable but also has a low specific-surface free energy comparable with those of the low-index MAJOR's of germanium[4] because surfaces far away from it, at least 7.8°, can still be facet to facets of it.

IV. THE MODEL

To tell if Si(20 4 23) is a MAJOR or a MINOR, we need to know if its unit cell is faceted to nanofacets of any MAJOR('s). Normally, this means that we need to know the atomic structure of the surface. Typical high-resolution STM images of the surface are then given in Fig. 4. A glancing can tell that the filled- and empty-state images are similar. Despite some less significant differences, the most eye-catching common feature of the two images is the troughs with some deeper pits. To interpret the STM features in terms of the surface atomic structure one must be very careful, as it has been known since the very beginning of STM that for semiconductor surfaces it is the local density of states (LDOS), instead of the surface geometry, that directly determine the STM features.[24] With this in mind, intuitively we would still believe that for surfaces with large-atomic corrugations it must be the surface geometry rather than the LDOS that dominates the STM features. In other words, the larger the surface-atomic corrugations are, the more the filled- and empty-state images are expected to be similar to each other. In fact, this idea finds strong support from the calculated STM images by Erwin and coworkers.[11,13] In the case of Si(5 5 12), the atomic corrugations are very large, meanwhile not only are the calculated filled- and empty-state images very similar to each other but also are the calculated images similar to their experimental counterpart very much.[11] However, in the case of Si(114), the atomic corrugations are much smaller and, not accidentally, none of these similarities can really be regarded as obvious.[13] Nevertheless, some differences do exist between the filled- and empty-state images of the Si(20 4 23) surface, indicating some contributions from the LDOS of the surface, and we hope it to be further reduced from the images. To reduce the LDOS contributions it has been suggested to use the averaged (or combined) image of a pair of filled- and empty-state images acquired simultaneously, instead of the two original images.[25] This idea is

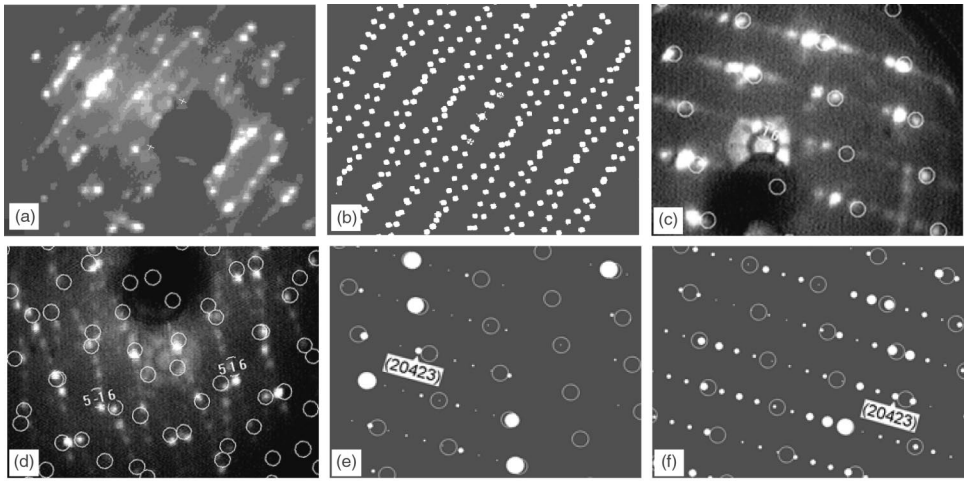

FIG. 2. (a) LEED pattern (30 eV) of the well-annealed Si(515) surface, which has two (0 0) spots marked with "+," showing that the surface is completely faceted [to understand this pattern, see (b)]. (b) Simulated LEED pattern (30 eV) of a Si(515) surface completely faceted to (20 4 23) and (23 4 20) facets with their (0 0) spots marked with "+." (c) LEED pattern (24 eV) of the well-annealed Si(516) surface, showing that the surface is completely faceted to facets of Si(20 4 23) 1×1. The white circles in this figure as well as those in (c) through (f) mark the spots of the Si{516 }1×1 surface(s). (d) LEED pattern (36 eV) of the well-annealed Si(405) surface, showing that the surface is completely faceted to facets of Si(20 4 23)1×1 and (20 −4 23)1×1. (e) LEED pattern (33 eV) of the truncated Si(20 4 23) surface [Fig. 5(a)], calculated under the kinematic approximation. (f) LEED pattern (33 eV) of the model surface [Fig. 5(c)] after Keating-type strain energy minimization, calculated also under the kinematic approximation.

supported by the results of the early paper of Tersoff and Hamann[24] as well as many recent works,[10,26] and has been used in our recent papers.[4] The combined image obtained from the pair of images in Figs. 4(a) and 4(b) is thus given in 4(c), and we shall start to build a model on the basis of it.

As always, we start from comparing the truncated surface [see Fig. 5(a)] with the combined image [see Fig. 4(c)] to find out the approximately required modification to the surface. The truncated surface consists of slightly tilted zigzag chains and thus can be viewed as a stepped (101) surface, where narrow (101) terraces are separated by steps running from lower left to upper right. As one can see, this morphology is essentially preserved in the image, except the troughs in the [1 −5 0] direction. In spite of this, the troughs are the major features of the surface as they can be clearly seen even in the low-magnification image given in Fig. 3(a). We believe that the zigzag chains are cut into segments by the troughs. Actually, it has been shown that in the case of Ge(101) the zigzag chains are cut into short segments, because long zigzag chains would cause strong local stresses and thus could not exist.[27] A model then has been proposed for the Si(20 4 23) surface and is schematically shown in Fig. 5(c). We can think of a two-step process from the truncated surface via Fig. 5(b) to the model as follows. First, we remove from Fig. 5(a) all surface atoms (that is, atoms with one or two dangling bonds) inside the shaded stripe and add a surface atom at every place indicated with the shaded circles so to get Fig. 5(b). Second, in each unit cell we let five of the seven chain-head atoms (that is, atoms with two dangling bonds) rebond, make the rest two a dimer, and put a $H_3$3 adatom *A* so to get the final model in Fig. 5(c). Thus the model has rebonded atoms, dimers, H_3 adatoms, and chain atoms as its building entities. Probably not acciden-

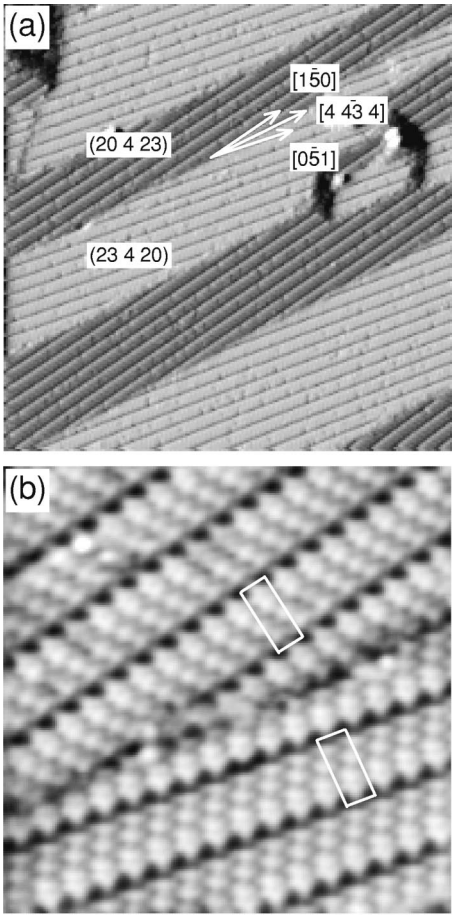

FIG. 3. STM images (ac mode, see text) acquired from the well-annealed Si(515) surface. (a) 1230 Å×1230 Å, −2.0 V, 5 pA. (b) With a (20 4 23) (upper) and (23 4 20) (lower) unit-cell outlined. 230 Å×230 Å, 1.2 V, 20 pA.

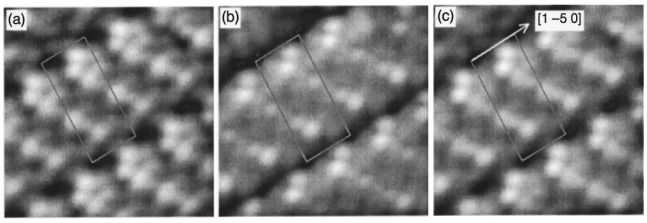

FIG. 4. High-resolution STM images (dc mode, 58 Å×58 Å, 20 pA) acquired from the well-annealed Si(515) surface, with a unit-cell outlined. (a) Filled-state image (−1.2 V). (b) Empty-state image (+1.2 V). (c) Combined image, that is, the average of the images in (a) and (b).

tally, all these building entities also exist in the Ge(101)$c(8\times10)$ surface.[27]

To show the agreement of the model with the experimental STM images, we have to calculate the simulated image from the model and, in turn, have to know the atomic coordinates of the model. For this purpose, we use the Keating-type strain-energy minimization scheme that was used with satisfaction for predicting atomic relaxations,[28] although the scheme cannot be used to compare the energetic of competing models and will never introduce structures like buckled dimers that break symmetry. In view of that the experimental images are determined mainly by the surface geometry, as we have just discussed, to calculate the simulated image from the model we simply calculate the convolution of the surface with the STM tip, which is approximated as a sphere with a radius of 4°, rather than the surface LDOS contours.[24] Moreover, as for Si and Ge surfaces STM can image essentially only those atoms carrying a dangling bond,[29] therefore we need to calculate the convolution of the tip with only such atoms. The calculated image of the model is given in Fig. 6. As one can see, the overall agreement between the calculated and experimental STM images is good, especially the position of the troughs and pits, thus supporting the model.

V. DISCUSSION

Now we discuss the justifications of the model. Apparently, dangling-bond reduction has to be of first consideration. The model has 36 dangling bonds (DB) per unit cell [see Fig. 5(c)] in contrast to 46 of the truncated surface [see Fig. 5(a)]. This equivalents to a density of 0.079 DB/Å^2, which is albeit slightly higher than 0.068 DB/Å^2 of Si(001)2×1 but very close to 0.077 DB/Å^2 of Si(313)12×1 (Ref. 19) and is much lower than 0.086 DB/Å^2 of Ge(101)$c(8\times10)$.[27] As mentioned, the most prominent and interesting feature of the surface is the troughs, which are clearly visible in the medium or even low magnification images (see Fig. 2). Obviously, the driving force behind the trough formation or cutting longer zigzag chains into short segments is relief of local-stress induced by dangling-bond reduction, rather than dangling-bond reduction itself, because without the troughs the model would have fewer dangling bonds. Actually, it has been suggested that the same driving force is responsible for the existence of only short-chain segments in the Ge(101)$c(8\times10)$ surface.[27] Apart from dangling-bond reduction and local-stress relief, the Si(20 4 23) surface apparently can have its charge redistributed so to further reduce the energy,[9] because it has four different types of building entities lying at different height levels and with their dangling bonds pointing to different directions.

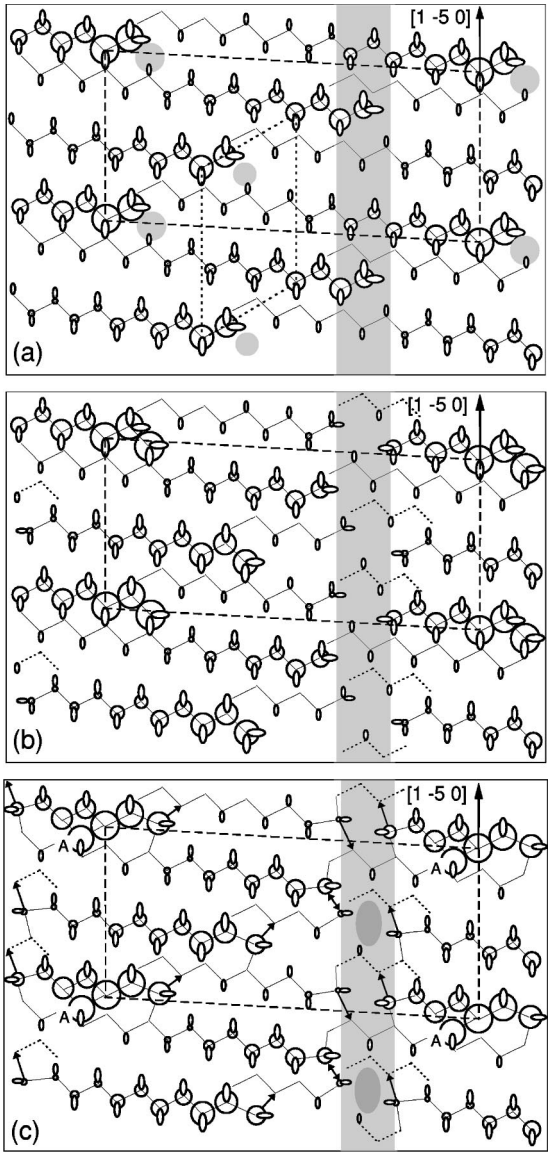

FIG. 5. (a) Schematic drawing of the truncated Si(20 4 23) surface, with the smaller circles representing atoms at the lower positions and the oblongs representing the dangling bonds and a unit cell ($\mathbf{a}$=32.8 Å, $\mathbf{b}$=13.8 Å, α_{ab}=93.8°) is outlined with the dashed lines, while a (516) unit cell is outlined with the dotted lines. (b) Schematic drawing of the intermediate surface obtained from (a) by removing all surface atoms (that is, atoms with one or two dangling bonds) inside the shaded stripe and adding a surface atom at every place indicated with the shaded circles. (c) Schematic drawing of the Si(20 4 23) model, with the two atoms of a dimer connected by a two-end arrow and the rebonded atoms carrying an arrow pointing to the atom to which they rebond. The shaded strip and oblongs mark the trough and pits, respectively.

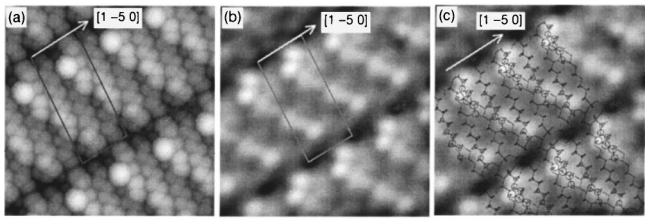

FIG. 6. (a) STM-image calculated from the model surface given in Fig. 5(c), with a unit-cell outlined. (b) The experimental image [same as Fig. 4(c)]. (c) Same as (b) but with the model superimposed. The $[1\ \ -5\ \ 0]$ direction is shown with an arrow.

At this point it is interesting to consider the common structural feature of the reconstructed Si(20 4 23), (313), and (101) surfaces. These surfaces are not far from each other in the stereographic triangle, as one can see from Fig. 1(b), and the surface atoms of their truncated surfaces form long zigzag chains. It has been known that the Si(101)''16×2'' surface consists of equally spaced but alternatively raised and lowered strips lying along the (112) direction,[30] that is, all zigzag chains are cut into short segments in the real surface, although the structural details of the surface are still in controversy.[27,31] Very recently, it has been pointed out not only that the long zigzag chains of the truncated Si(313) surface do not exist in the real Si(313)12×1 surface either but also that the surface is highly corrugated in the atomic scale.[19] Now, we have just seen the model proposed for the Si(20 4 23)1×1 surface. Although it is only for further investigations and some details of it may need modifications or may even be incorrect, there should be no doubt that the long zigzag chains of the truncated surface must be also cut into short segments by the troughs in the real surface. In view of these, we reach the conclusion that long zigzag chains of surface atoms are energetically too costly to exist, and this is true not only for Ge(101) (Ref. 27) and (313) (Ref. 32) but also for Si(101),[30] (313),[19] and (20 4 23) and hence for silicon and germanium surfaces in general. This implies that except cutting long zigzag chains of surface atoms into short segments there are no easy ways to eliminate them, such as putting adatoms between neighboring chains as suggested previously.[31,33]

Looking at the LEED patterns given in Fig. 2 carefully, it is not difficult to find that in all three studied cases the {20 4 23} LEED spots are brighter when they are near a {516} LEED spot [marked with a white circle in Figs. 2(a), (c), and (d)]. It should be emphasized that this does not mean that the Si(20 4 23) unit cell is faceted to (516) nanofacets, because the situation is different from that in the case of Si(105).[18] To show this, using kinematic approximation, we calculated the LEED patterns of the truncated and model surfaces. The spots of the calculated pattern of the truncated surface [see Fig. 2(e)] are bright only when they are very close to a (516) spot, as one would expect, because (20 4 23) is only 1.2° away from (516) and thus a unit cell of the truncated (20 4 23) surface mainly consists of three (516) unit cells. On the other hand, in the calculated pattern of the model [see Fig. 2(f)] although the brighter spots still tend to appear around a (516) spot but no longer have to be very close to it, indicating that the model (20 4 23) unit cell contains a (516) nanofacet, which is smaller than that in the truncated unit cell. This is an obvious feature of the model, as one can see from Fig. 5(c). Comparing this pattern with the experimental pattern of, say, the faceted (516) surface [see Fig. 2(c)], one can find that they are very similar, in the sense that the brighter spots tend to appear around a (516) spot albeit not have to be very close to it. This fact, in addition to the STM images given in Fig. 6, further supports the model. Obviously, there is no step-bunching involved in the model. In other words, *the unit cell of the* (20 4 23) *surface is not faceted* and hence the surface is, by definition, *a major stable surface*.

Finally, we would like to point out that the well-annealed Si(515) surface, which has a very nice grating-like morphology with a ''period'' of about 50 nm [see Fig. 3(a)], may be used as templates for growth of ''quantum-wire'' nanostructures. One advantage of this kind of templates is that they are thermodynamically stable, rather than in a dynamic steady state, as in the case of stress-induced templates.[7] Apparently, to avoid the facets other than (20 4 23) and (23 4 20) from appearing [see in Fig. 3(a)] so to grow ''infinitely'' long wires, one may use Si(43 8 43), which is 0.6° away from (515) towards (101) but still belongs to the same zone of (20 4 23) and (23 4 20); while to get templates with an asymmetric cross section or a smaller depth one may use surfaces belonging to the same zone but between (43 8 43) and (20 4 23). Besides, the troughs of the Si(20 4 23) surface, which form a gratinglike structure with a period of 32.8 Å, may also be used as templates to grow nanowires.

VI. SUMMARY

In summary, STM and LEED observations show that Si(515), (516), and (405) are unstable as after being well annealed they are faceted to {20 4 23} facets and thus that Si(20 4 23) is a stable surface. On the basis of the high-resolution dual-bias images along with analysis of the LEED pattern, Si(20 4 23) is further identified as a MAJOR because its unit cell is not faceted to nanofacets of any other stable surfaces but has its own structure. Interestingly, among all seven MAJOR's of silicon that have been found so far (20 4 23) is the only one that silicon does not share with germanium. A detailed model has been proposed for the atomic structure of the Si(20 4 23) 1×1 surface for further investigation.

Considering what exist in the well-annealed Si(20 4 23), Si(313),[19] Si(101),[30,31] Ge(101),[27] and Ge(313) (Ref. 32) surfaces are only short zigzag chains of surface atoms whereas what exist in their truncated counterpart are long ones, we reach the conclusion that the long ones are energetically too costly to exist. Moreover, the fact that these surfaces are all very corrugated in the atomic scale indicates that except cutting the long zigzag chains into short segments there are no easy ways to eliminate them, such as putting adatoms between neighboring chains as previously suggested.[31,33]

Silicon surfaces between (20 4 23) and (43 8 43), after being well annealed, may be used as templates with a variable cross section to grow ''quantum wire'' nanostructures, as these surfaces can facet to (20 4 23) and (23 4 20) nano-

facets, which can self-assemble into a very nice thermodynamically stable grating-like structure.

ACKNOWLEDGMENTS

Jinlong Jiang and Li Zhou are acknowledged for their involvement in the analysis of the LEED patterns. Jianbang Chen of the Beijing General Research Institute for nonferrous metals is acknowledged for preparation of the samples. Z.G. thanks the Japan Society for the Promotion of Science (JSPS) for providing her with financial support. This work was supported by the National Natural Science Foundation of China (under Grant No. 19634010) and the special funding from the Education Ministry of China.

*Author to whom correspondence should be addressed. Electronic address: wsyang@pku.edu.cn

[1] F.M. Ross, R.M. Tromp, and M.C. Reuter, Science **286**, 1931 (1999).
[2] H. Omi and T. Ogino, Phys. Rev. B **59**, 7521 (1999).
[3] S.G.J. Mochrie, S. Song, M.R. Yoon, D.L. Abernathy, and G.B. Stephenson, Physica B **221**, 105 (1996); A.A. Baski, S.C. Erwin, and L.J. Whitman, Surf. Sci. **392**, 69 (1997).
[4] Zheng Gai, W.S. Yang, R.G. Zhao, and T. Sakurai, Phys. Rev. B **59**, 15230 (1999), and the references therein.
[5] S.Y. Shiryaev, F. Jensen, J.L. Hansen, J.W. Peterson, and A.N. Larsen, Phys. Rev. Lett. **78**, 50 (1997).
[6] P.W. Murray, I.M. Brookes, S.A. Haycock, and G. Thornton, Phys. Rev. Lett. **80**, 988 (1998).
[7] Feng Liu, J. Tersoff, and M.G. Lagally, Phys. Rev. Lett. **80**, 1268 (1998).
[8] Zheng Gai, W.S. Yang, T. Sakurai, and R.G. Zhao, Phys. Rev. B **59**, 13009 (1999).
[9] D. Haneman, Rep. Prog. Phys. **50**, 1045 (1987); J.P. LaFemina, Surf. Sci. Rep. **16**, 133 (1992).
[10] J. Dabrowski, H.-J. Mü ssig, and G. Wolff, Phys. Rev. Lett. **73**, 1660 (1994).
[11] A.A. Baski, S.C. Erwin, and L.J. Whitman, Science **269**, 1556 (1995).
[12] A.A. Baski and L.J. Whitman, Phys. Rev. Lett. **74**, 956 (1995).
[13] S.C. Erwin, A.A. Baski, and L.J. Whitman, Phys. Rev. Lett. **77**, 687 (1996).
[14] Jian Wei, E.D. Williams, and R.L. Park, Surf. Sci. Lett. **250**, L368 (1991); H. Tanaka, Y. Watanabe, and I. Sumita, Appl. Surf. Sci. **76/77**, 340 (1994).
[15] W.E. Packard and J.D. Dow, Phys. Rev. B **55**, 15643 (1997); M. Menon, N.N. Lathiotakis, and A.N. Andriotis, *ibid.* **56**, 1412 (1997).
[16] B.Z. Olshanetski and V.I. Mashanov, Surf. Sci. **111**, 414 (1981).
[17] Zheng Gai, W.S. Yang, R.G. Zhao, and T. Sakurai, Phys. Rev. B **59**, 13003 (1999).
[18] R. G. Zhao, Zheng Gai, Wenjie Li, Jinlong Jiang, Y. Fujikawa, T. Sakurai, and W. S. Yang, (unpublished).
[19] Zheng Gai, R.G. Zhao, T. Sakurai, and W.S. Yang, Phys. Rev. B **63**, 085301 (2000).
[20] Zheng Gai *et al.* (unpublished).
[21] W.S. Yang, X.-D. Wang, K. Cho, J. Kishimoto, T. Hashizume, and T. Sakurai, Phys. Rev. B **51**, 7571 (1995).
[22] R.G. Zhao, J.F. Jia, and W.S. Yang, Phys. Rev. B **48**, 5333 (1993).
[23] B.Z. Olshanetsky and A.A. Shklyaev, Surf. Sci. **82**, 445 (1979).
[24] J. Tersoff and D.R. Hamann, Phys. Rev. B **31**, 805 (1985).
[25] Zheng Gai, H. Ji, B. Gao, R.G. Zhao, and W.S. Yang, Phys. Rev. B **54**, 8593 (1996).
[26] U.J. Knall *et al.*, Phys. Rev. Lett. **66**, 1733 (1991); J.H. Wilson *et al.*, Ultramicroscopy **42-44**, 801 (1992); M. Tsukada *et al.*, Surf. Sci. Rep. **13**, 265 (1991); H. Kageshima *et al.*, Phys. Rev. B **46**, 6928 (1992); J. Wang *et al.*, *ibid.* **47**, 10326 (1993).
[27] Zheng Gai, R.G. Zhao, and W.S. Yang, Phys. Rev. B **57**, R6795 (1998).
[28] R.M. Tromp and E.J. Van Loenen, Surf. Sci. **155**, 441 (1985); J.S. Pedersen, *ibid.* **210**, 238 (1989).
[29] H. Neddermeyer, Rep. Prog. Phys. **59**, 701 (1996).
[30] H. Ampo, S. Miura, K. Kato, Y. Ohkawa, and A. Tamura, Phys. Rev. B **34**, 2329 (1986); E.J. van Loenen, D. Dijkkamp, and A.J. Hoeven, J. Microsc. **152**, 487 (1988).
[31] W.E. Packard and J.D. Dow, Phys. Rev. B **55**, 15643 (1997).
[32] Zheng Gai, R.G. Zhao, and W.S. Yang, Phys. Rev. B **58**, R4223 (1998).
[33] B.Z. Olshanetsky, S.A. Teys, and I.G. Kozhemyako, Phys. Low-Dimens. Semicond. Struct. **11/12**, 85 (1998).